Enhanced Insulin-Stimulated Activation of Phosphatidylinositol 3-Kinase in the Liver of High-Fat–Fed Rats

Motonobu Anai, Makoto Funaki, Takehide Ogihara, Akira Kanda, Yukiko Onishi, Hideyuki Sakoda, Kouichi Inukai, Masao Nawano, Yasushi Fukushima, Yoshio Yazaki, Masatoshi Kikuchi, Yoshitomo Oka, and Tomoichiro Asano

Insulin receptor substrate (IRS)-1 and IRS-2, which mediate phosphatidylinositol (PI) 3-kinase activation, play essential roles in insulin-induced translocation of GLUT4 and in glycogen synthesis. In this study, we investigated the process of PI 3-kinase activation via binding with IRS-1 and -2 in liver, muscle, and fat of high-fat–fed rats, a model of insulin-resistant diabetes. In the liver of high-fat–fed rats, insulin increased the PI 3-kinase regulatory subunit p85α and the PI 3-kinase activities associated with IRS-1 3.6- and 2.4-fold, and with IRS-2, 4.7- and 3.0-fold, respectively, compared with those in control rats. The tyrosine phosphorylation levels of IRS-1 and IRS-2 were not significantly altered, however. In contrast with the liver, tyrosine phosphorylation levels and associated PI 3-kinase proteins and activities were decreased in the muscle and adipose tissue of high-fat–fed rats. Thus, high-fat feeding appears to cause insulin resistance in the liver by a mechanism different from the impaired PI 3-kinase activation observed in muscle and adipose tissue. Taking into consideration that hepatic PI 3-kinase activation is severely impaired in obese diabetic models such as Zucker fatty rats, it is possible that the mechanism by which a high-fat diet causes insulin resistance is quite different from that associated with obesity and overeating due to abnormality in the leptin system. This is the first report to show increased PI 3-kinase activation by insulin in an insulin-resistant diabetic animal model. These findings may be important for understanding the mechanism of insulin resistance in human NIDDM, since a high-fat diet is considered to be one of the major factors exacerbating insulin insensitivity in humans. *Diabetes* 48:158–169, 1999

From the Third Department of Internal Medicine (M.F., T.O., A.K., Y.On., H.S., M.N., Y.F., Y.Y., T.A.), Faculty of Medicine, University of Tokyo, Tokyo; the Institute for Adult Diseases (M.A., K.I., M.K.), Asahi Life Foundation, Tokyo; and the Third Department of Internal Medicine (Y.Ok.), Yamaguchi University School of Medicine, Ube, Japan.

Address correspondence and reprint requests to Tomoichiro Asano, MD, 7-3-1 Hongo, Bunkyo-ku, Tokyo, 113, Japan. E-mail: asano-tky@umin.ac.jp.

Received for publication 22 October 1997 and accepted in revised form 17 September 1998.

ECL, enhanced chemiluminescence; HGP, hepatic glucose production; IRS, insulin receptor substrate; PBS, phosphate-buffered saline; PI, phosphatidylinositol; R_d, rate of plasma glucose disappearance; R_a, rate of plasma glucose appearance; R_g', glucose metabolic index.

NIDDM is characterized by a strong genetic background. It is also agreed, however, that the acquired factors inducing insulin resistance play a critical role on the occurrence and progression of NIDDM. Several factors, such as obesity, hypertension, hyperlipidemia (1), administration of dexamethasone (2–5), and insufficient physical exercise (6–8), are believed to contribute to insulin resistance. In terms of nutritional factors in the diet, high-fat content (9–12), alcohol (13), and fructose (14) lead to insulin resistance.

Phosphatidylinositol (PI) 3-kinase has been shown to be essential for insulin signaling with respect to the metabolic effect of insulin. In muscle and adipose tissue, PI 3-kinase is considered to be important for insulin-induced glucose uptake via the translocation of GLUT4 from the intracellular membrane to the plasma membrane (15–17). Furthermore, the activation of PI 3-kinase was reported to play an important role in insulin-induced glycogen synthesis and suppression of phosphoenolpyruvate carboxykinase expression in hepatocytes (18–23). Thus, impaired insulin signaling leading to insufficient activation of PI 3-kinase could be a cause of insulin resistance. In fact, many studies have shown the insulin-induced activation of PI 3-kinase to be decreased in liver, muscle, and epididymal fat in a number of diabetic rodent models (24–28), as well as in muscles of obese humans (29).

The aim of this study was to determine the impaired step in insulin signaling in the liver, muscle, and adipose tissue of high-fat–fed rats. First, we investigated the mRNA and protein expression levels of insulin receptor substrate (IRS)-1, IRS-2, the PI 3-kinase regulatory subunit, and the PI 3-kinase catalytic subunit. Second, we investigated insulin-induced tyrosine phosphorylations of IRS-1 and IRS-2, the amounts of PI 3-kinase regulatory subunit associated with IRS-1 and IRS-2, and PI 3-kinase activities associated with IRS-1 and IRS-2. We show hepatic PI 3-kinase activation to be markedly enhanced in high-fat–fed rats compared with control rats, while being suppressed in muscle and epididymal fat.

RESEARCH DESIGN AND METHODS

Animals. Male Sprague-Dawley rats were purchased from Tokyo Experimental Animals (Tokyo, Japan) at 5 weeks of age. After a 2- to 3-day acclimatization period, the rats were divided into a normal diet group and a high-fat diet group and fed ad libitum for 2 or 6 weeks. All experiments were performed using a 2-week high-fat diet group and control group, if not indicated otherwise. The high-fat diet

consisted of 58% lard (wt/wt), 30% fish powder, 10% skim milk, and a 2% vitamin and mineral mixture (equivalent to 7.5% carbohydrate, 24.5% protein, and 60% fat). The normal diet proportions were 54% carbohydrate, 20% protein, and 4.5% fat.

Hyperinsulinemic-euglycemic clamp. After 14 days on the respective diets, the rats were anesthetized with pentobarbital sodium (50 mg/kg) intraperitoneally, and the left jugular vein and left femoral vein were catheterized. The jugular and femoral catheters were used for blood sampling and infusion, respectively, during the clamp.

Euglycemic-hyperinsulinemic clamp was performed as described previously (30). Briefly, 3 mU · kg^{-1} · min^{-1} human insulin (Novolin R, Novo Nordisk, Denmark) was continuously infused for 2 h; this rate produces insulin levels of a submaximal response. The blood glucose concentration was clamped at 100 mg/dl by estimating blood glucose concentration at 5-min intervals in samples taken from the jugular vein and adjusting the rate of infusion of 20% glucose solution delivered via the femoral cannula. The glucose infusion rate during the 2nd hour of the clamp was taken as the response parameter of the potency of whole-body insulin action. Blood samples (0.2 ml) were obtained for insulin determination in all studies at 0, 60, and 120 min.

In vivo insulin action in individual tissues. The nonmetabolizable glucose analogs 2-deoxy-D-[1-^{3}H]glucose (50 μCi) and D-[U-^{14}C]glucose (50 μCi) (NEN Life Science Products, Boston,MA) were administered together as an intravenous bolus at 75 min after the commencement of the study. Blood samples (150 μl) for determination of blood and plasma glucose concentrations and plasma tracer concentrations were obtained at 2, 5, 10, 15, 20, 30, and 45 min after bolus administration. At the completion of the clamp, the soleus muscle and epididymal fat pad were removed and frozen in liquid nitrogen. An estimate of tissue glucose uptake (defined as the glucose metabolic index, R_g'), the rates of plasma glucose disappearance (R_d) and appearance (R_a) were calculated as previously described (30).

In vivo insulin stimulation. Food was withdrawn 12–14 h before the experiments. Rats were anesthetized with pentobarbital sodium (60 mg/kg body wt) intraperitoneally, and the abdominal cavity was opened. The portal vein was exposed, and 4 ml normal saline (0.9% NaCl) with or without 10^{-5} mol/l insulin were injected after blood sampling. The livers were removed 30 s later, and the hindlimb skeletal muscle and epididymal fat were removed 90 s later and immediately homogenized in a 6× volume of homogenization buffer A (1% Triton X-100, 50 mmol/l HEPES [pH 7.4], 100 mmol/l sodium pyrophosphate, 100 mmol/l sodium fluoride, 10 mmol/l EDTA, 10 mmol/l sodium vanadate, 2 mmol/l phenylmethylsulfonyl fluoride, and 0.1 μg/ml aprotinin) with a polytron operated at maximum speed for 30 s. Both extracts were centrifuged at 15,000*g* at 4°C for 30 min to remove insoluble material, and the supernatants were used as samples for immunoprecipitation or immunoblotting.

Immunoprecipitation and immunoblotting. Supernatants containing equal amounts of protein were incubated with anti–IRS-1 (10 μg/ml), anti–IRS-2 (10 μg/ml) (31), anti-phosphotyrosine (4G10) (10 μg/ml), anti-p85α (UBI), anti-p85β (10 μg/ml) (32), anti-p110α (10 μg/ml), or anti-p110β (10 μg/ml) (33) antibodies and incubated with 10 μl protein A-Sepharose 6MB. Anti–Grb-2 antibody was purchased from Medical and Biological Laboratories, Nagano, Japan.

The samples were washed five times with phosphate-buffered saline (PBS) and boiled in Laemmli sample buffer containing 100 mmol/l dithiothreitol. Total lysates or immunoprecipitated proteins (10 μg) were subjected to SDS-PAGE (6 or 10% Tris acrylamide). Electrotransfer of proteins from the gel to nitrocellulose filters was performed for 3 h at 90 V (constant), immunoblotting with each of the aforementioned antibodies was performed with enhanced chemiluminescence (ECL), and band intensities were quantified with a Molecular Imager GS-525 using Imaging Screen-CH.

Activity of PI 3-kinase. After insulin injection into the portal vein, portions of the liver and hindlimb muscles were removed and immediately homogenized as previously described (33). The homogenates were subjected to centrifugation at 15,000*g* for 30 min at 4°C, and the supernatants were used as samples. IRS-1, IRS-2, and tyrosine phosphorylated proteins were immunoprecipitated from aliquots of the supernatant containing 10 mg protein with anti–IRS-1, anti–IRS-2, or 4G10 antibodies, respectively, followed by protein A-Sepharose 6MB. The assays of PI 3-kinase activity in the immunoprecipitates were performed as previously described (33).

RNA extraction. Total tissue RNA was isolated using an Isogen RNA isolation kit (Nippon Gene, Toyama, Japan). RNA concentrations were estimated based on absorbance at 260 nm. Total RNA in 4-μg aliquots was electrophoresed in 1% agarose gel, stained with ethidium bromide, and examined visually to confirm quality and integrity and to estimate RNA extract quantities.

Preparation of riboprobes. The riboprobe for PI 3-kinase regulatory subunits p50α, p55α, p55γ, p85α, and p85β, catalytic subunits p110α and p110β, and IRS-1 and IRS-2 were prepared as previously described (33).

The riboprobe was synthesized according to the manufacturer's instructions (T3/T7 in vitro transcription system; Clontech Laboratories, Palo Alto, CA). Linearized plasmid DNA (1 μg) was used as a template and labeled in vitro with [α-^{32}P]UTP (~800 Ci/mmol/l; Amersham Japan, Tokyo). After DNase I treatment, the samples were electrophoresed through 5% polyacrylamide/8 mol/l urea gels which were then exposed to X-ray film. The fragment at the positive signal was excised, and the riboprobe was eluted by incubation at 37°C in 5 mol/l ammonium acetate.

RNase protection assay. RNase protection assays were performed according to the manufacturer's instructions (RPA II; Ambion, Austin, TX). Pooled samples of 10 μg total RNA from liver or 20 μg total RNA from muscle in each group were mixed with molar excesses of ^{32}P-labeled probe (8×10^4 cpm) and incubated overnight at 44°C. Single-stranded RNA was removed by digestion with RNase A/RNase T1 for 30 min at 37°C. Protected fragments were precipitated and electrophoresed on 5% polyacrylamide/8 mol/l urea gel, which was then analyzed using a Molecular Imager GS-525 (Nippon Bio-Rad Laboratories KK, Tokyo).

Statistical analysis. All experimental data are expressed as means ± SE. Statistical analysis was performed with paired or unpaired two-tailed Student's *t* tests. $P < 0.05$ was considered significant.

RESULTS

Characterization of high-fat–fed rats. Table 1 summarizes the body weight, food intake, blood glucose, serum insulin, and serum triglyceride data from the high-fat–fed and control rats. There was no significant difference in body weight between the control and high-fat–fed rats before the experiment. By 2 weeks, the body weights of high-fat–fed rats had slightly but significantly increased compared with those of control rats ($P < 0.05$). Food intakes, calculated as daily caloric intake, did not differ between control and high-fat–fed rats. Blood glucose and serum triglyceride levels were increased in high-fat–fed rats ($P < 0.01$, $P < 0.05$, respectively). Fasting serum insulin did not differ between control and high-fat–fed rats.

In vivo insulin resistance in high-fat–fed rats. In vivo insulin action was measured using the euglycemic glucose clamp technique in rats at insulin infusion rates designed to achieve submaximal stimulation of overall glucose disposal rate (3 mU · kg^{-1} · min^{-1}) and suppression of hepatic glucose production (HGP).

The high-fat diet was effective in inducing both peripheral and hepatic insulin resistance (Table 2). Glucose disposal rate during submaximal insulin infusion in the fat-fed group was 28% less than that in the diet-fed control group (27.1 ± 1.7 vs. 19.5 ± 1.2, $P < 0.001$). During submaximal insulin infusion, the ability of insulin to suppress hepatic glucose production (HGP) was impaired in the high-fat–fed group. In submaximal insulin infusion rates, HGP was 220% greater in the high-fat–fed group compared with the control group (3.8 ± 1.8 vs. 12.3 ± 1.7, $P < 0.001$).

As shown in Fig. 1, glucose metabolic index in soleus muscle and epididymal fat pad was also impaired in the high-

TABLE 1
Characterization of high-fat–fed rats

	Normal diet	High-fat diet
Body weight (g)		
Initial	123 ± 2	125 ± 1
Final	261 ± 4	289 ± 9*
Energy intake (cal/day)	96	97
Fasting blood glucose (mmol/l)	3.5 ± 0.3	4.8 ± 0.2†
Fasting serum insulin (pmol/l)	122 ± 6	121 ± 9
Fasting triglyceride (mg/dl)	66 ± 8	233 ± 80*

Data are means or means ± SE. Significantly different from diet-fed rats: *$P < 0.05$, †$P < 0.01$.

TABLE 2
Amounts of PI 3-kinase regulatory and catalytic subunit mRNA and protein in liver, muscle, and epididymal fat of high-fat–fed rats

	Liver		Muscle		Fat	
	Normal diet	High-fat diet	Normal diet	High-fat diet	Normal diet	High-fat diet
p85α						
mRNA	100 ± 22	74 ± 20	100 ± 10	76 ± 12		
Protein	100 ± 6	109 ± 6	100 ± 5	102 ± 3	100 ± 5	90 ± 7
p85β						
mRNA	100 ± 26	95 ± 3	100 ± 1	122 ± 6*		
Protein	100 ± 6	115 ± 11	100 ± 7	132 ± 17	100 ± 16	141 ± 15
p55α						
mRNA	100 ± 31	113 ± 26	100 ± 7	91 ± 3		
Protein	100 ± 8	141 ± 21*	100 ± 5	81 ± 8†	Undetectable	
p55γ						
mRNA	100 ± 6	77 ± 6	100 ± 27	89 ± 5		
Protein	Undetectable		Undetectable		Undetectable	
p50α						
mRNA	100 ± 30	134 ± 10	Undetectable			
Protein	100 ± 6	102 ± 7	Undetectable		Undetectable	
p110α						
mRNA	100 ± 20	71 ± 11	100 ± 10	112 ± 4		
Protein	100 ± 8	114 ± 10	100 ± 24	81 ± 19	100 ± 7	91 ± 7
p110β						
mRNA	100 ± 21	83 ± 5	100 ± 2	112 ± 31		
Protein	100 ± 10	104 ± 9	100 ± 15	66 ± 4*	100 ± 12	121 ± 10

Data are means ± SE. Significantly different from rats fed a normal diet: *P < 0.05, †P < 0.02.

fat–fed group compared with the control group. R_g' in muscle and epididymal fat pad was decreased by 50 and 74%, respectively, in the high-fat–fed group compared with the control group. These results indicate that high-fat feeding induces insulin resistance not only in muscle and adipose tissue, but also in liver.

IRS-1 and -2 mRNA levels in liver and muscle of high-fat–fed rats. The amounts of IRS-1 mRNA were revealed to be unchanged both in liver and muscle of rats on the high-fat diet, compared with those of rats on the normal diet (Fig. 2*A* and *B*). The IRS-2 mRNA level in high-fat–fed rat liver was decreased to 55% of that in control rats, while no significant difference was observed in the muscle IRS-2 mRNA level between the two groups (Fig. 2*F* and *G*).

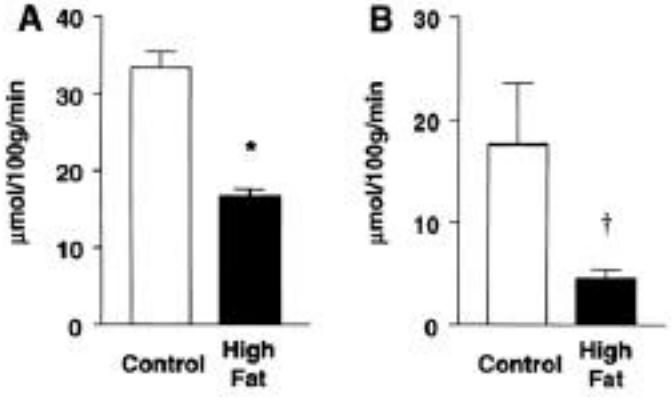

FIG. 1. Insulin-stimulated glucose metabolic index (R_g') (n = 4–6) in tissues of control and high-fat diet rat groups. □, control diet rats; ■, high-fat–fed rats. *A*: Soleus muscle. *B*: Epididymal fat. *P < 0.0001, †P < 0.05, high-fat–fed rats versus controls.

IRS-1 and -2 protein levels in liver, muscle, and adipose of high-fat–fed rats. The amounts of IRS-1 protein in the liver and muscle of high-fat–fed rats were shown to be very similar to those of control rats (Fig. 2*C* and *D*). In contrast, the IRS-1 protein level in the adipose tissue of the high-fat–fed rats was decreased to 55% of that in control rats (Fig. 2*E*).

Similar results were obtained for IRS-2 protein levels. The IRS-2 protein level was significantly downregulated in the adipose tissue of high-fat–fed rats (by 35%) compared with controls (Fig. 2*J*), while the IRS-2 protein levels in liver and muscle were not significantly altered by high-fat feeding (Fig. 2*H* and *I*).

Tyrosine phosphorylation levels of IRS-1 in liver, muscle, and epididymal fat. Because impaired tyrosine phosphorylation of IRS-1 and IRS-2 after insulin stimulation has been observed in many diabetic animal models, we investigated the tyrosine phosphorylation level of IRS-1 and -2 in liver, muscle, and epididymal fat. Basal hepatic tyrosine phosphorylation levels of IRS-1 were similar in controls and high-fat–fed rats (Fig. 3*A*). With in vivo insulin stimulation, tyrosine phosphorylation levels of IRS-1 in the livers of high-fat–fed rats were shown to be increased by 38% compared with control rats, but the difference was not statistically significant (Fig. 3*A*).

Basal muscle tyrosine phosphorylation levels of IRS-1 were similar in control and high-fat–fed rats (Fig. 3*B*). In the insulin-stimulated state, however, the tyrosine phosphorylation levels of IRS-1 in high-fat–fed rats were reduced to 58% of those in control rats (Fig. 3*B*, P < 0.05).

The tyrosine phosphorylation levels of IRS-1 in the adipose tissue of high-fat–fed rats were decreased to 43% of the control level, possibly reflecting the reduced IRS-1 protein levels

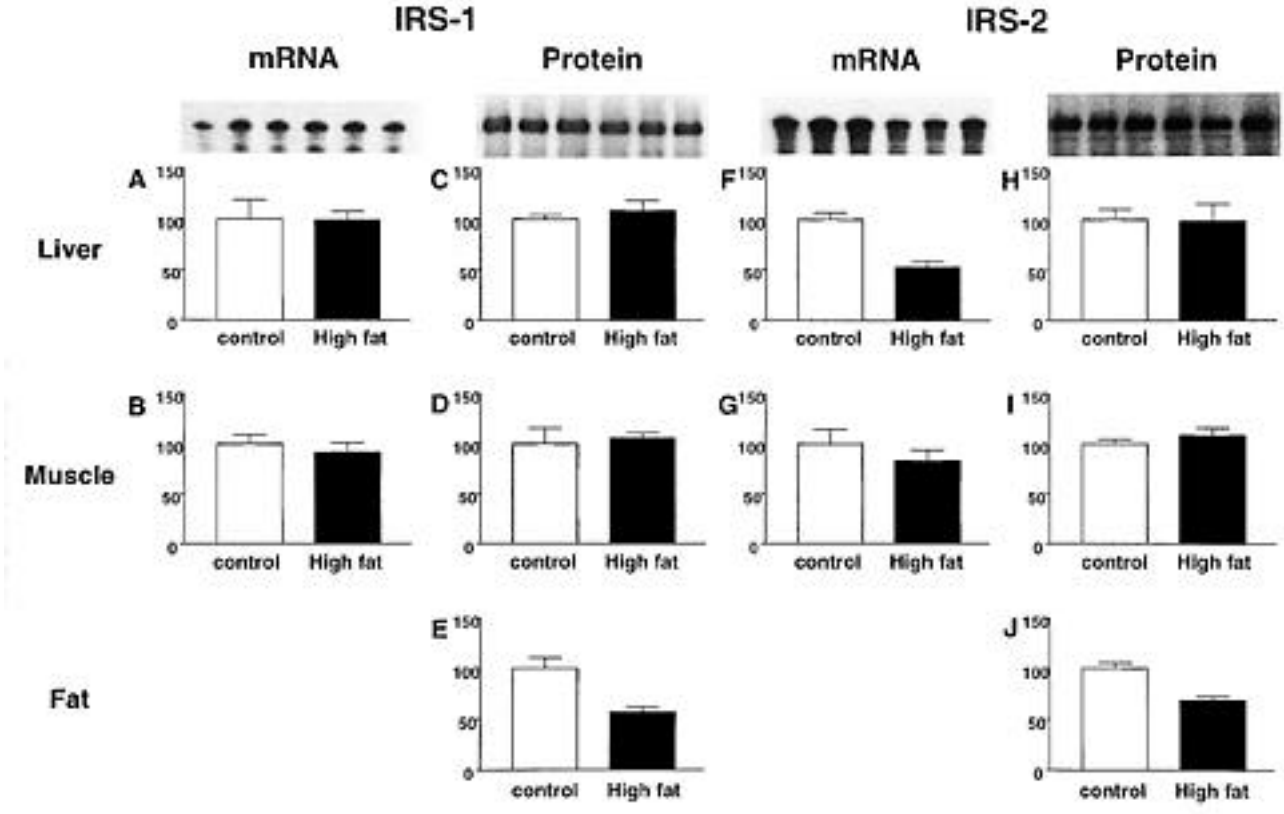

FIG. 2. The amounts of mRNA and protein of IRS-1 and -2 in liver, muscle, and epididymal fat of high-fat–fed rats. RNA in liver and muscle and proteins in liver, muscle, and epididymal fat were isolated as described in METHODS. Aliquots of total RNA (5 µg for liver, 10 µg for muscle) were used for RNase protection assays with radiolabeled antisense riboprobes for IRS-1 and IRS-2 mRNAs. Protected fragments were resolved on 5% polyacrylamide urea gel and subjected to autoradiography, and RNase-protected band intensities were analyzed with a Molecular Imager. The IRS-1 and -2 protein amounts were determined by immunoprecipitation and immunoblotting with the respective antibodies. The images show RNase-protected bands or immunoreactive proteins from the livers of three control and three high-fat–fed rats. The bar graph represents quantitation of the results of three independent experiments. Results are indicated as percent of control. *A*: IRS-1 mRNA in liver. *B*: IRS-1 mRNA in muscle. *C*: IRS-1 protein in liver. *D*: IRS-1 protein in muscle. *E*: IRS-1 protein in epididymal fat. $P < 0.01$ high-fat–fed rats vs. control. *F*: IRS-2 mRNA in liver. $P < 0.01$ high-fat–fed rats vs. control. *G*: IRS-2 mRNA in muscle. *H*: IRS-2 protein in liver. *I*: IRS-2 protein in muscle. *J*: IRS-2 protein in epididymal fat. $P < 0.001$ high-fat–fed rats vs. control. ND, not determined.

in epididymal fat. Tyrosine phosphorylation of IRS-1 after insulin stimulation in rats on the high-fat diet was reduced to 72% of those in control rats (Fig. 3*C*).

Tyrosine phosphorylation levels of IRS-2 in liver, muscle, and epididymal fat. Basal tyrosine phosphorylation levels of hepatic IRS-2 were similar in control and high-fat–fed rats. After in vivo insulin stimulation, the tyrosine phosphorylation levels of IRS-2 in high-fat–fed rats were 85% of those in the control rats, but the difference was not statistically significant (Fig. 3*D*).

Basal tyrosine phosphorylation levels of muscle IRS-2 were slightly increased in high-fat–fed rats. The insulin-induced increase in tyrosine phosphorylation of muscle IRS-2 in high-fat–fed rats was decreased to 66% ($P < 0.05$) of the control level (Fig. 3*E*).

The basal adipose tissue tyrosine phosphorylation levels of IRS-2 were slightly, but significantly, increased in high-fat–fed rats compared with control rats (Fig. 3*F*, $P < 0.05$). In the insulin-stimulated state, the phosphorylation of IRS-2 was markedly suppressed in the adipose of rats on the high-fat diet, to 46% of that in control rats (Fig. 3*F*). Thus, IRS-2 phosphorylation was suppressed in muscle, and even more markedly in epididymal fat, but not in the liver.

Effects of high-fat diet on p85α associated with IRS-1 in liver, muscle, and epididymal fat. After phosphorylation of IRS-1 by insulin, p85α noncovalently binds with IRS-1 via the SH2 domain. To evaluate the amount of p85α bound with tyrosine phosphorylated IRS-1, we performed immunoblotting using the antibody against p85α in the IRS-1 immunoprecipitates. Surprisingly, in the livers of high-fat–fed rats, even in the basal state, ~10 times more p85α was associated with IRS-1 than in control rats (Fig. 4*A*). After insulin stimulation, the amount of p85α associated with hepatic IRS-1 in high-fat–fed rats increased to 3.6-fold the amount in control rat livers (Fig. 4*A*, $P < 0.01$).

In muscle, in the basal state, the levels of p85α associated with IRS-1 were similar in control and high-fat–fed rats (Fig. 4*B*). After insulin stimulation, although the levels were increased in both groups, the amount of p85α associated with IRS-1 in high-fat–fed rats was significantly decreased to 78% of that in control rats (Fig. 4*B*, $P < 0.02$).

In epididymal fat, in the basal state, p85α binding with IRS-1 in high-fat–fed rats was reduced to 65% of that in the control rats, not statistically significant (Fig. 4*C*). In the insulin-stimulated state, the amount of p85α associated with IRS-1 in high-fat–fed rats was significantly reduced, to 74% of

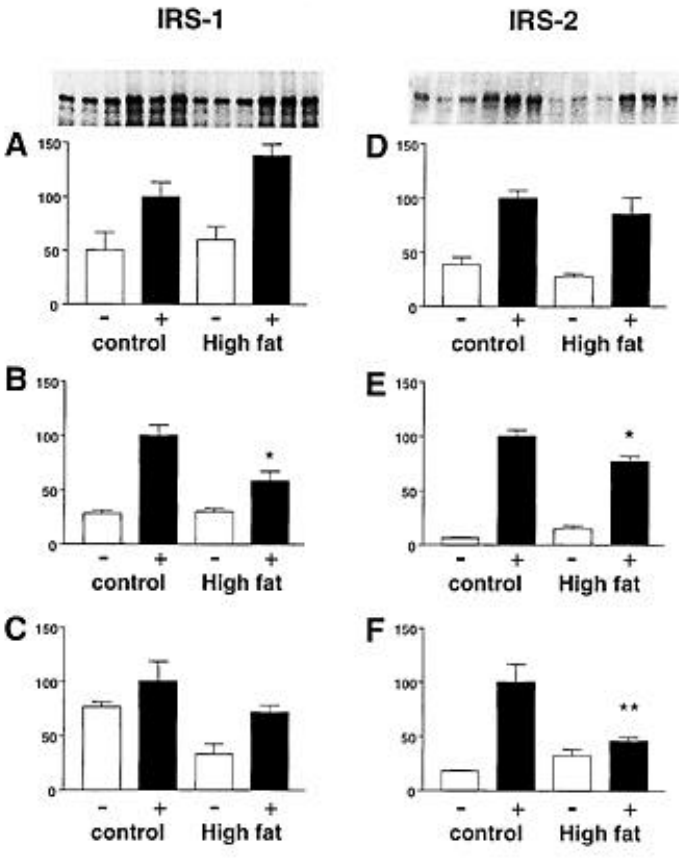

FIG. 3. Tyrosine phosphorylation of IRS-1 and -2 in the liver, muscle, and epididymal fat of high-fat–fed rats. Rats were anesthetized, and the abdominal wall was incised to expose the viscera. Normal saline or saline with 10^{-5} mol/l insulin (4 ml) was injected into the portal vein as a bolus; 30 s later, livers were excised; 90 s later, hindlimb skeletal muscle and epididymal fat were excised. All tissues were immediately homogenized in extraction buffer at 4°C as described in METHODS. After centrifugation, aliquots with the same amount of protein were immunoprecipitated with anti–IRS-1 or anti–IRS-2 antibodies at 4°C and subsequently with protein A-Sepharose. Immunoprecipitated proteins were immunoblotted with 4G10 using ECL. The quantitation was performed with a Bio-Rad Molecular Imager. The images show immunoreactive proteins from the livers of three control rats with and three without insulin stimulation, and from three high-fat–fed rats with and three without insulin stimulation. The bar graph represents quantitation of the results of three independent experiments. Results are presented as percent of control. Tyrosine phosphorylation of IRS-1 in liver (A), muscle (B), and epididymal fat (C) and of IRS-2 in liver (D), muscle (E), and epididymal fat (F). Significant differences from control: *P < 0.05, **P < 0.02.

that in control rats (Fig. 4*C*, $P < 0.02$). Thus, the amount of p85α associated with IRS-1 after insulin stimulation was markedly increased in the liver while being decreased in muscle and epididymal fat, reflecting differences in regulation in different tissues.

Effects of high-fat diet on p85α associated with IRS-2 in liver, muscle, and epididymal fat. In the basal state, the amount of p85α associated with IRS-2 in the liver of high-fat–fed rats was significantly increased, by threefold, compared with the amount in control rat liver (Fig. 4*D*). In addition, the amount of p85α associated with hepatic IRS-2 after insulin stimulation was 4.6 times higher in high-fat–fed than in control rats (Fig. 4*D*, $P < 0.01$).

In muscle, the basal level of p85α associated with IRS-2 in high-fat–fed rats was decreased to 68% of that in control rats (Fig. 4*E*). In the insulin-stimulated state, the level in muscle of high-fat–fed rats was decreased to 77% of that in control rats (Fig. 4*E*, $P < 0.02$).

In epididymal fat, the basal amount of p85α associated with IRS-2 in high-fat–fed rats was decreased to 67% of that in control rats (Fig. 4*F*). After insulin stimulation, the level of p85α binding with IRS-2 in high-fat–fed rats was decreased to 54% of that in control rats, and the increase above the basal amount was decreased by 69% compared with the control level (Fig. 4*F*, $P < 0.01$).

Effect of high-fat diet on the amount of p85α associated with 4G10 immunoprecipitates. In the basal state, the amount of p85α in 4G10 immunoprecipitates from the high-fat–fed rat liver was increased by 133% compared with the control level (Fig. 4*G*). With insulin stimulation, the amount in the high-fat–fed rat liver was 151% of the control level (Fig. 4*G*, $P < 0.05$).

The amounts of p85α associated with 4G10 immunoprecipitates in muscle, in the basal state, were similar in control and high-fat–fed rats (Fig. 4*H*). In the insulin-stimulated state, the amount of bound p85α in high-fat–fed rats was significantly decreased to 73% of that in control rats (Fig. 4*H*, $P < 0.001$).

In the basal state, the amounts of p85α associated with 4G10 immunoprecipitates were similar in the epididymal fat of high-fat–fed and control rats (Fig. 4*I*). After insulin stimulation, however, these amounts were significantly increased in both groups, the amount in high-fat–fed rats being 61% of that in control rats (Fig. 4*I*, $P < 0.05$).

Effects of high-fat diet on PI 3-kinase activities associated with IRS-1 in liver, muscle, and adipose tissue of high-fat–fed rats. In the liver of high-fat–fed rats, basal PI 3-kinase activity associated with IRS-1 was six times higher than that in control rats (Fig. 5*A*). PI 3-kinase was significantly increased by insulin stimulation in both groups. The insulin-stimulated increase in high-fat–fed rats was remarkable, reaching 234% of the control rat liver level (Fig. 5*A*, $P < 0.01$).

Without insulin stimulation, PI 3-kinase activities associated with IRS-1 in muscle were similar in high-fat–fed and control rats (Fig. 5*B*). PI 3-kinase activity associated with IRS-1 after insulin stimulation was significantly decreased in high-fat–fed rats, to 67% of the control level (Fig. 5*B*, $P < 0.05$).

PI 3-kinase activation by insulin was also decreased in epididymal fat of high-fat–fed rats. Without insulin stimulation, PI 3-kinase activity associated with IRS-1 in high-fat–fed rats was similar to that in control rats (Fig. 5*C*). After insulin stimulation, activities were increased ninefold and fourfold in control and high-fat–fed rats, respectively, the nearly 50% decrease in the latter being statistically significant (Fig. 5*C*, $P < 0.005$).

Effects of high-fat diet on PI 3-kinase activities associated with IRS-2 in liver, muscle, and adipose tissue. In liver, PI 3-kinase activity associated with hepatic IRS-2 was increased, as in the IRS-1 immunoprecipitates. Without insulin stimulation, PI 3-kinase activity associated with hepatic IRS-2 in high-fat–fed rats was seven times that in control rats (Fig. 5*D*). After insulin stimulation, PI 3-kinase activity associated with hepatic IRS-2 in high-fat–fed rats was increased to 200% of that in control rats (Fig. 5*D*, $P < 0.001$).

In muscle, without insulin stimulation, PI 3-kinase activity associated with IRS-2 was only slightly increased in high-

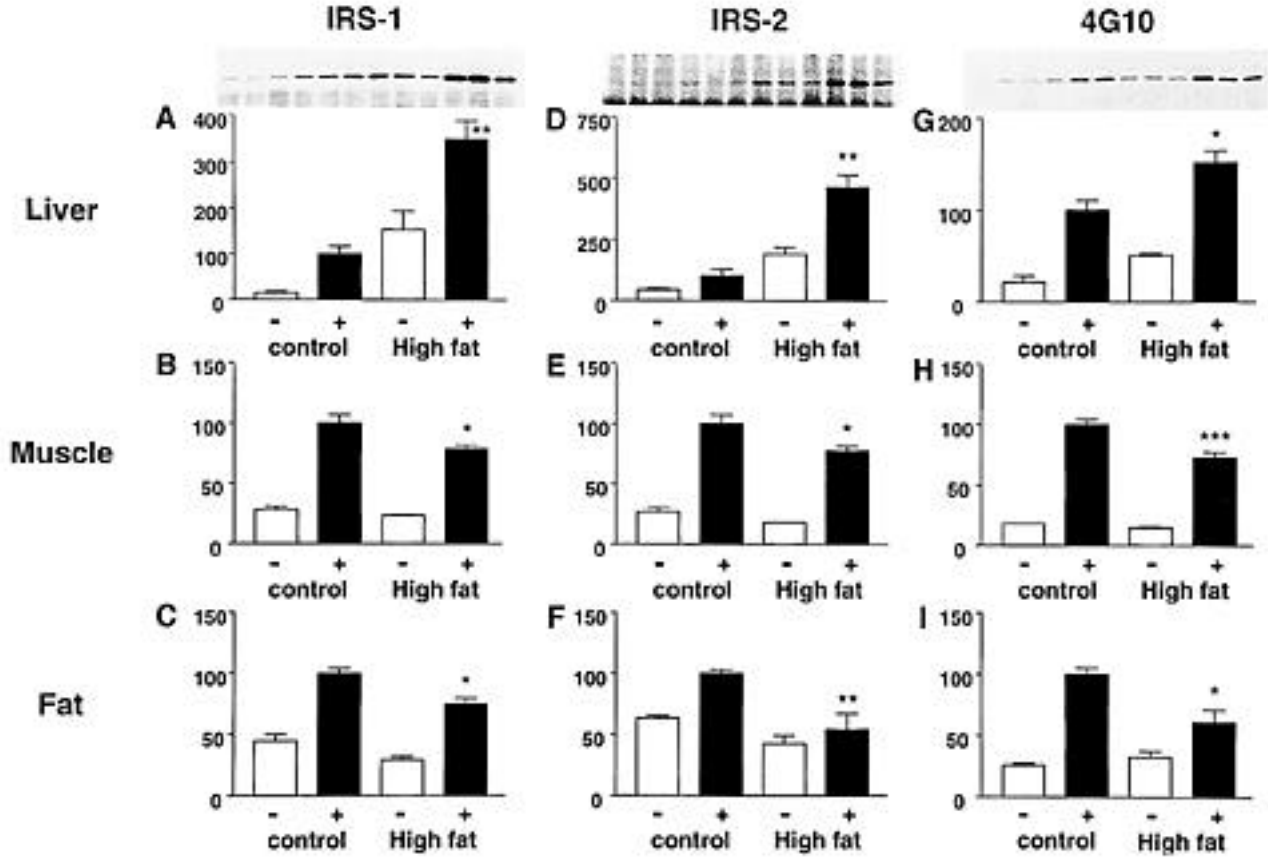

FIG. 4. The amounts of PI 3-kinase (p85α subunit) associated with IRS-1, IRS-2, and tyrosine phosphorylated proteins in liver, muscle, and epididymal fat. The immunoprecipitated proteins were prepared as described in Fig. 2. The immunoprecipitated proteins were used for immunoblotting with anti-p85α antibodies using ECL. Results were quantitated with a Bio-Rad Molecular Imager. The images show immunoreactive proteins from the livers of three control rats with and three without insulin stimulation, and from three high-fat–fed rats with and three without insulin stimulation. The bar graph represents quantitation of the results of three independent experiments. Results are presented as percent of control. p85α associated with IRS-1 in liver (*A*), muscle (*B*), and epididymal fat (*C*), with IRS-2 in liver (*D*), muscle (*E*), and epididymal fat (*F*), and with 4G10 in liver (*G*), muscle (*H*), and epididymal fat (*I*). Significant differences from control: **P* < 0.05, ***P* < 0.01, ****P* < 0.001.

fat–fed rats compared with control rats (Fig. 5*E*). After insulin stimulation, PI 3-kinase activity associated with IRS-2 in high-fat–fed rats was reduced to 83% of that in control rats, not a significant decrease (Fig. 5*E*).

In epididymal fat, PI 3-kinase activity associated with IRS-2 was decreased in a manner similar to that observed in IRS-1 immunoprecipitates. Without insulin stimulation, the activity in epididymal fat of high-fat–fed rats was similar to that in control rats (Fig. 5*F*). PI 3-kinase activity in high-fat–fed rats, after insulin stimulation, was decreased to 42% of that in control rats, and the increase above the basal level was only 24% of that in control rats (Fig. 5*F*, $P < 0.0001$).

Effects of high-fat diet on PI 3-kinase activities associated with anti-phosphotyrosine antibody immunoprecipitates in liver, muscle, and epididymal fat. As in the anti–IRS-1 and anti–IRS-2 immunoprecipitates, we investigated the PI 3-kinase activity associated with anti-phosphotyrosine antibody immunoprecipitates. Without insulin stimulation, PI 3-kinase activity associated with 4G10 immunoprecipitates from the liver of high-fat–fed rats was twice the control rat level (Fig. 5*G*). In the insulin-stimulated state, PI 3-kinase activity associated with 4G10 immunoprecipitates in high-fat–fed rats was increased to 168% of the control level (Fig. 5*G*, $P < 0.01$).

Without insulin stimulation, PI 3-kinase activity associated with 4G10 immunoprecipitates from muscle of high-fat–fed rats was decreased to 81% of the control level (Fig. 5*H*). The absolute value of muscle PI 3-kinase activity in high-fat–fed rats when stimulated with insulin was significantly decreased, to 70% of that in control rats (Fig. 5*H*, $P < 0.0001$).

Without insulin stimulation, PI 3-kinase activity associated with 4G10 immunoprecipitates from epididymal fat of high-fat–fed rats was decreased to 84% of the control level (Fig. 5*I*). After insulin stimulation, the PI 3-kinase activity in high-fat–fed rats was markedly suppressed, to 42% of the control level (Fig. 5*I*, $P < 0.05$).

Effect of 6 weeks of high-fat feeding on PI 3-kinase activity in liver, muscle, and epididymal fat. To investigate the long-term effect of high-fat feeding on insulin signaling, we measured the PI 3-kinase activity of liver, muscle, and epididymal fat after 6 weeks of high-fat feeding. As shown in Fig. 6, PI 3-kinase activity in liver was increased, whereas that in muscle and epididymal fat pad was decreased. Especially in liver, PI 3-kinase activity in the basal

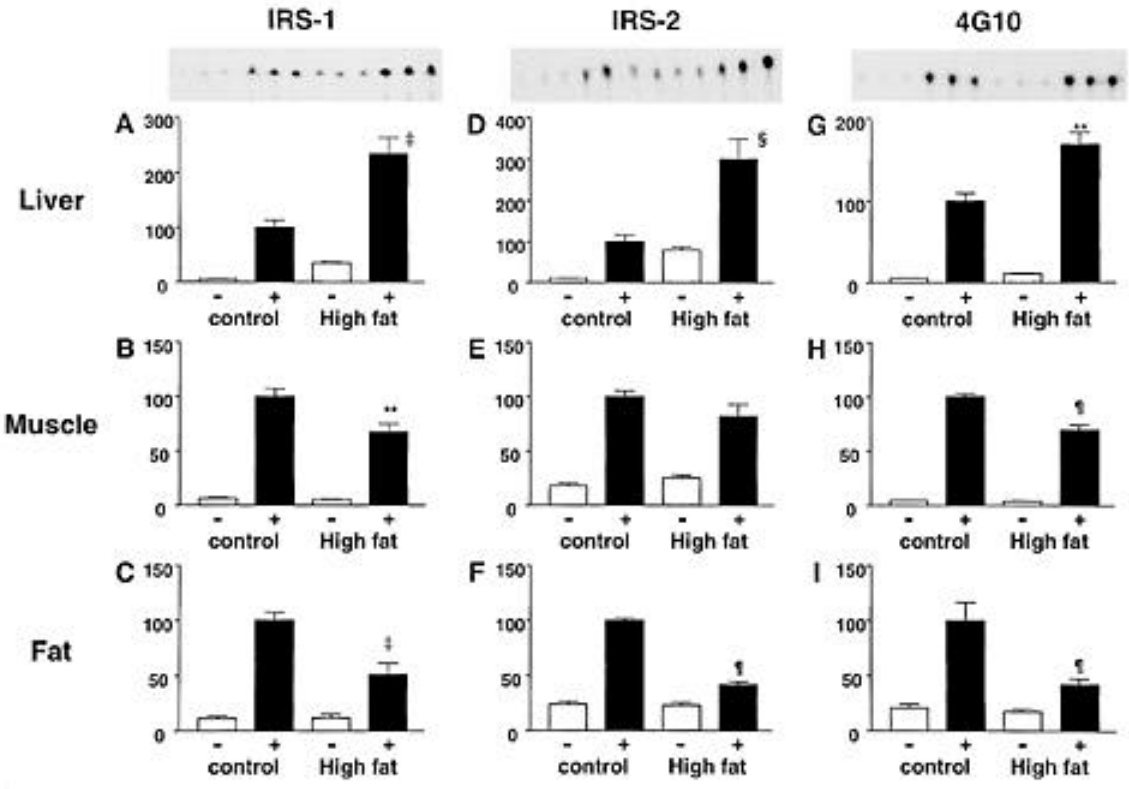

FIG. 5. PI 3-kinase activities associated with IRS-1, IRS-2, and tyrosine phosphorylated proteins in liver, muscle, and epididymal fat of high-fat–fed rats. Liver, muscle, and epididymal fat homogenates were immunoprecipitated with anti–IRS-1, anti–IRS-2 or 4G10 antibodies. PI 3-kinase activities in the immunoprecipitates were assayed as described in METHODS. The resulting labeled lipids were extracted, separated by thin-layer chromatography, and quantitated and visualized with a Bio-Rad Molecular Imager. The images show PI 3-phosphate from the livers of three control rats without and three with insulin stimulation, and from three high-fat–fed rats without and three with insulin stimulation. The bar graph represents quantitation of the results of three independent experiments. Results are presented as percent of control. PI 3-kinase activities associated with IRS-1 in liver (A), muscle (B), and epididymal fat (C); with IRS-2 in liver (D), muscle (E), and epididymal fat (F); and with 4G10 immunoprecipitates in liver (G), muscle (H), and epididymal fat (I). Significant differences from control: **$P < 0.01$, ‡$P < 0.005$, §$P < 0.0005$, ¶$P < 0.0001$.

state in high-fat–fed rats was similar to or greater than that in the insulin-stimulated state in control rats. Insulin-stimulated hepatic PI 3-kinase activity after 6 weeks of high-fat diet was around three to five times that of control rats. Compared with the results shown in Fig. 5, the increase in hepatic PI 3-kinase activity was progressive in high-fat–fed rats.

Effect of high-fat diet on expression levels of PI 3-kinase regulatory subunit in liver, muscle, and epididymal fat. Various regulatory subunit isoforms reportedly exhibit different PI 3-kinase activity–elevating responses to insulin (32). Thus, altered expression levels of PI 3-kinase regulatory subunits might contribute to impaired insulin signaling.

Table 2 summarizes the amounts of PI 3-kinase regulatory and catalytic subunit mRNA and protein. Liver, muscle, and epididymal fat p85α expression levels in high-fat–fed rats were similar to those in control rats. Hepatic p85β mRNA and protein levels were similar in high-fat and control diets. mRNA of p85β in muscle of high-fat–fed rats was increased by 22% compared with the control level ($P < 0.05$). Although not significantly different, the level of protein expression was 32% higher than in control rats. p85β expression in epididymal fat was not significantly different.

p55α is an alternative splicing form of p85α, most abundantly expressed in brain but also present in various other tissues. The level of hepatic mRNA of p55α in high-fat–fed rats did not differ significantly from that in control rats. Protein expression, however, was 41% higher in high-fat–fed than in control rats ($P < 0.05$). p55α mRNA was slightly decreased—by 9%—in muscle of high-fat–fed rats compared with the control level. Expression of p55α protein was significantly reduced, to 81% of the control level ($P < 0.02$). Thus, p55α expression is regulated differently in liver and muscle of high-fat–fed rats.

p55γ is expressed most abundantly in brain and testes. mRNA of this isoform was detected in liver and muscle, and p55γ expressions were slightly lower in the high-fat–fed rats than in the control rats. Expression, as determined by the RNase protection assay, was weak, and insulin-stimulated activity of PI 3-kinase regulated through this isoform was barely detectable. Thus, the reductions appeared to have little effect on insulin signaling in this animal model.

p50α is an alternative splicing form of p85α, expressed most abundantly in the liver, and has six unique amino acids in its NH_2-terminus (32). mRNA of p50α in the liver of high-fat–fed rats was increased by 34% compared with the control, not a statistically significant difference. The expressions of p50α protein were similar in the two groups. Neither p50α mRNA nor protein was detected in muscle, because of the very low level of p50α expression.

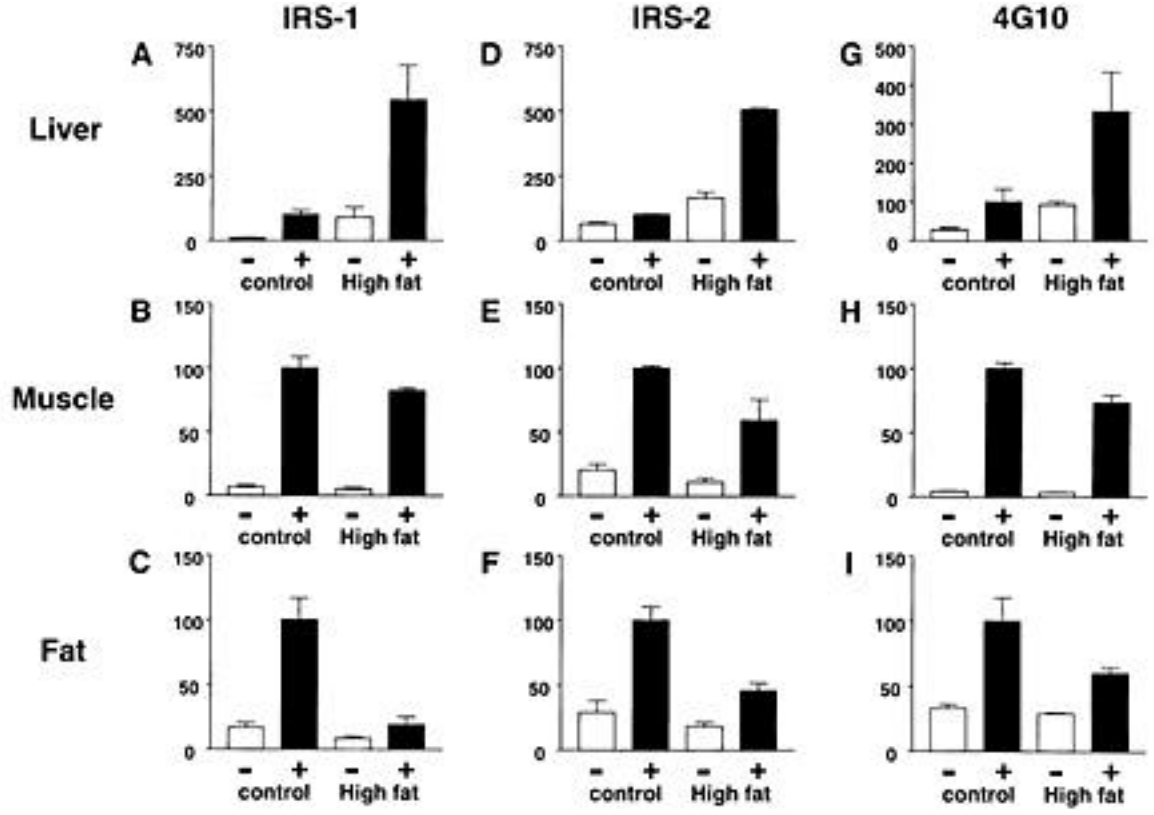

FIG. 6. PI 3-kinase activities associated with IRS-1, IRS-2, and tyrosine phosphorylated proteins in liver, muscle, and epididymal fat of rats fed high-fat diets for 6 weeks. Liver, muscle, and epididymal fat homogenates were immunoprecipitated with anti–IRS-1, anti–IRS-2, or 4G10 antibodies. PI 3-kinase activities in the immunoprecipitates were assayed as described in METHODS. The resulting labeled lipids were extracted, separated by thin-layer chromatography, and quantitated and visualized with a Bio-Rad Molecular Imager. The bar graph represents quantitation of the results of three independent experiments. Results are presented as percent of control. PI 3-kinase activities associated with IRS-1 in liver (*A*), muscle (*B*), and epididymal fat (*C*); with IRS-2 in liver (*D*), muscle (*E*), and epididymal fat (*F*); and with 4G10 immunoprecipitates in liver (*G*), muscle (*H*), and epididymal fat (*I*).

Effects of high-fat diet on expressions of PI 3-kinase catalytic subunit in liver, muscle, and epididymal fat. mRNA of p110α in the livers of high-fat–fed rats was decreased to 71% of that in control rats, while the level of p110α protein expression was similar to that in control rats. Expression of p110α in muscle and epididymal fat pad of the high-fat–fed rats was not significantly different.

p110β mRNA and protein expressions in the livers of high-fat–fed rats were not significantly different. In muscle, mRNA expression in high-fat–fed rats was similar to that in controls, while protein expression was decreased to 66% of the control level ($P < 0.05$). p110β protein expression in epididymal fat of high-fat–fed rats was not significantly different.

Effect of high-fat diet on insulin-stimulated binding of Grb-2 with IRS-1 in liver and epididymal fat. To explore the mechanism of increased p85α binding with IRS-1 without increased phosphorylation of IRS-1, Grb-2 binding with IRS-1 was investigated in the liver and epididymal fat pad of high-fat diet and control rats.

As shown in Fig. 7, Grb-2 binding with IRS-1 in liver and epididymal fat pad was increased by insulin. Grb-2 associated with IRS-1 was increased in insulin-stimulated conditions in the liver of high-fat–fed rats by 120% compared with control diet rats. In contrast, Grb-2 associated with IRS-1 in epididymal fat pad was decreased by 50% compared with control. Thus, the high-fat diet–induced alteration of the binding of Grb-2 with IRS-1, in both the liver and adipose tissue, was revealed to be similar to that of p85α with IRS-1.

DISCUSSION

Peripheral insulin resistance in muscle, liver, and adipose tissue is a major component of NIDDM (34). Many environmental factors, such as obesity, stress, high-fat diet, and insufficient physical exercise, result in the development of insulin resistance (6–11). Many studies have been performed with the aim of elucidating the molecular events contributing to this impaired insulin sensitivity. To date, based on studies using various diabetic rodent models, insufficient insulin-induced PI 3-kinase activation appears to be common, although the degree of impairment of PI 3-kinase activation differs among models (24,26–28). As mentioned above, PI 3-kinase has been shown to be essential for insulin signaling, which modulates the metabolic effect of insulin in muscle and adipose tissue as well as in the liver (15,16,35–37). In addition, impaired PI 3-kinase activation is also reportedly present in the muscle tissue of obese humans (29). Thus, it is likely that the early steps in insulin signaling, preceding the activation of PI 3-kinase, account for a substantial portion of the molecular mechanism causing insulin resistance in NIDDM.

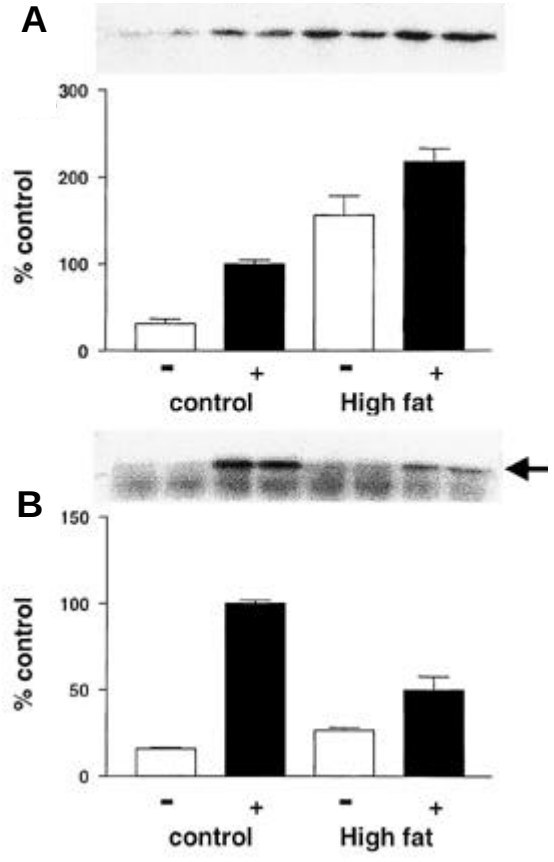

FIG. 7. The amounts of Grb-2 associated with IRS-1 in liver and epididymal fat. The immunoprecipitated proteins were prepared as described in Fig. 2. The immunoprecipitated proteins were used for immunoblotting with anti–Grb-2 antibodies using ECL. Results were quantitated with a Bio-Rad Molecular Imager. The images show immunoreactive proteins from two control rats with and two without insulin stimulation, and from two high-fat–fed rats with and two without insulin stimulation. The bar graph represents quantitation of the results of three independent experiments. Results are presented as percent of control.

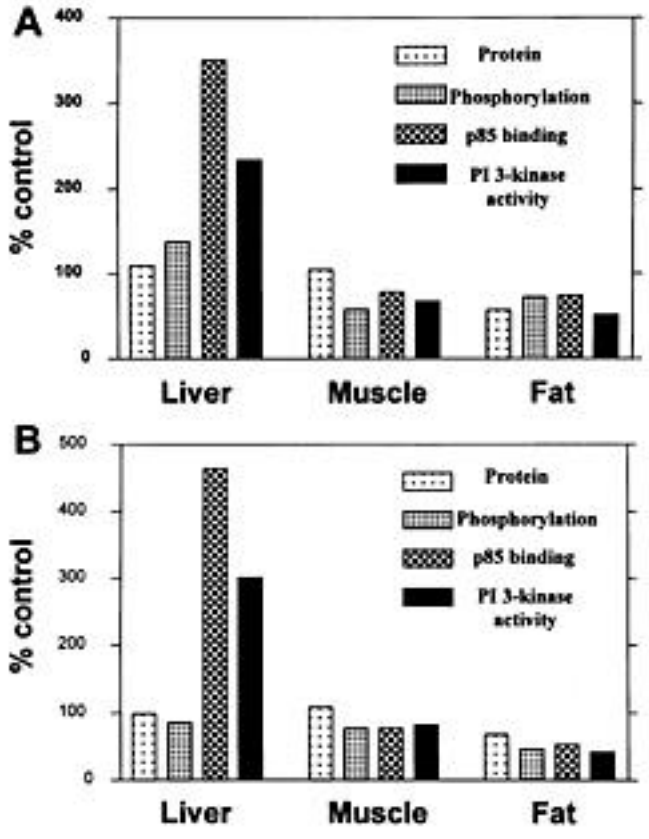

FIG. 8. Impaired steps in the IRS-1 and -2 pathways mediating insulin signaling. *A*: IRS-1. *B*: IRS-2. Protein, percent control of IRS-1 or IRS-2 protein levels in high-fat–fed rats. Phosphorylation, percent control of insulin-stimulated tyrosine phosphorylation of IRS-1 or IRS-2 in high-fat–fed rats. p85 binding, percent control of p85α binding associated with IRS-1 or IRS-2 after insulin stimulation in high-fat–fed rats. PI 3-kinase activity, percent control of PI 3-kinase activities associated with IRS-1 or IRS-2 in high-fat–fed rats.

To date, many studies have shown that insulin action is impaired in liver, muscle, and adipose tissue of high-fat–fed rats (10,38–44). For example, in high-fat–fed rats, basal HGP is increased, and insulin-stimulated suppression of HGP is impaired (39,42). Glycogen synthesis has been shown to be decreased in both muscle (10) and liver (43) with high-fat feeding. Insulin-induced glucose uptake and GLUT4 translocation to the plasma membrane were reported to be reduced in muscle and adipose tissues (41,44). Thus, it is apparent that a high-fat diet leads to insulin resistance in all three tissues. In fact, we confirmed that suppression of HGP by insulin and the glucose metabolic index of muscle and epididymal fat pad were impaired in our high-fat–fed rats.

Our findings of impaired PI 3-kinase activation in muscle and adipose tissue of high-fat–fed rats are in good agreement with those of previous reports (24,26,28). In contrast, insulin-induced PI 3-kinase activation was demonstrated to be markedly enhanced in the liver of high-fat–fed rats in our study. Similarly altered insulin-induced PI 3-kinase activation responses in these three tissues were also observed in rats fed a high-fat diet for 6 weeks, but the degrees were shown to be a little more marked compared with those for 2 weeks. Thus, the altered PI 3-kinase activation is not temporary only in the early period of high-fat induced insulin resistance, but is constitutionally observed in the late phase.

The expression levels of hepatic IRS-1 and IRS-2 were not shown to be significantly altered. In addition, the tyrosine phosphorylation levels of hepatic IRS-1 and IRS-2 were shown to be only slightly altered. The apparent change in hepatic insulin signaling was observed to be present at the step at which the p85α regulatory subunit of PI 3-kinase associates with IRS-1 and -2 (Fig. 8).

Poor nutrition reportedly alters expression of PI 3-kinase protein in the fetus (45). In addition, it has been reported that different PI 3-kinase regulatory subunits have different responses to insulin (32,46). Thus, we investigated how the expression levels of all five regulatory subunits and the two catalytic subunits are regulated in the tissues of high-fat–fed rats. The series of assays shown in Table 3 revealed that the PI 3-kinase expression level is not markedly altered in the high-fat–fed rat liver. In addition, we observed that binding of p50α with IRS-1 was increased in the liver of high-fat–fed rats similarly to that of p85α, by measuring the amount of hepatic IRS-1 in the anti-p50α and anti-p85α immunoprecipitates (data not shown). There-

TABLE 3
Hyperinsulinemic-euglycemic clamp data and effect of high-fat feeding on endogenous hepatic glucose output in response to submaximal insulin

	Control diet	High-fat diet
Plasma insulin (pmol/l)	558 ± 60	543 ± 64
Blood glucose (mmol/l)	5.6 ± 0.2	5.8 ± 0.1
Glucose infusion rate ($mg \cdot kg^{-1} \cdot min^{-1}$)	26.2 ± 0.7	11.1 ± 1.2*
R_d ($mg \cdot kg^{-1} \cdot min^{-1}$)	27.1 ± 1.7	19.5 ± 1.2†
R_a ($mg \cdot kg^{-1} \cdot min^{-1}$)	3.8 ± 1.8	12.3 ± 1.7‡

Data are means ± SE. Significantly different from control rats in same experiment: *$P < 0.0001$, †$P < 0.001$, ‡$P < 0.001$.

fore, despite neither tyrosine phosphorylation levels of IRS-1 and -2 nor the PI 3-kinase expression level being significantly increased, IRS-1– and -2–associated PI 3-kinase protein, very probably irrespective of the isoform of regulatory subunit, is markedly increased in the high-fat–fed rat liver.

IRS-1 and -2 contain ~20 putative tyrosine phosphorylation sites, only four of which are in the Y(M/X)XM motif reported to be responsible for the interaction with the regulatory subunits of PI 3-kinase (47,48). On the other hand, IRS-1 possesses two binding motifs with which Grb-2 reportedly associates. Our results indicated that not only p85α, but also Grb-2 binding with hepatic IRS-1, was upregulated by high-fat feeding in both the basal and insulin-stimulated states. IRS-1 and -2 also contain more than 30 potential serine/threonine phosphorylation sites for casein kinase II, protein kinase C, MAP kinase, and cdc2, as well as cAMP- and cGMP-dependent protein kinase phosphorylation sites (49). Thus, it is reasonable to speculate that a change in the phosphorylation level at any of these serine/threonine residues could alter the phosphorylation of specific tyrosine residues and thereby the ability of p85α and Grb-2 to bind with IRS-1 and -2. If such a mechanism exists, we can speculate that these sites become more heavily tyrosine phosphorylated in IRS-1 and -2 in the liver of high-fat–fed rats, while most of the other tyrosine residues or those recognized efficiently by anti-phosphorylation antibody are normally phosphorylated. Alternatively, the possibility cannot be excluded that the amount of the PI 3-kinase regulatory subunit or Grb-2 associated with IRS-1 and -2 is increased because of an unknown modification of the p85α or Grb-2 protein, such as via serine/threonine phosphorylation, which can be speculated based on previous reports (50,51). Further studies are necessary to clarify this issue.

Interestingly, in the liver of other obese diabetic rodent models, such as *ob*/*ob* mice (24) and Zucker fatty rats (33), PI 3-kinase activity associated with IRS-1 and -2 was found to be severely impaired when stimulated with insulin. In the case of Zucker fatty rats, which exhibit mild diabetes with marked hyperinsulinemia, tyrosine phosphorylation of IRS-1/2 is moderately impaired (to ~60–70% of the control level), and the associated PI 3-kinase activity is markedly decreased (to 10–20% of the control level) (33). Thus, the effect of the high-fat diet on insulin-induced PI 3-kinase activation was clearly shown to be opposite that of obesity induced by overeating, that is, that due to an abnormality of the leptin system. In the liver of high-fat–fed rats, the step from which the impaired insulin action originates may be downstream from PI 3-kinase activation.

On the other hand, we have demonstrated that neither IRS-1 nor IRS-2 protein levels were reduced in the muscle of high-fat–fed rats, and that the IRS-1 and IRS-2 phosphorylation step was impaired in those rats (Fig. 8). Both the amount of p85α protein and the PI 3-kinase activity associated with IRS-1 and -2 were decreased in the muscle of high-fat–fed rats, which can be explained by the decreased tyrosine phosphorylation of IRS-1 and -2.

Finally, in the case of epididymal fat, IRS-1 and -2 protein expression levels were shown to be reduced by 30–40% compared with the control level. These decreases in IRS-1 and -2 proteins caused decreases of the tyrosine phosphorylation level, the association of p85α protein with IRS-1 and -2, and PI 3-kinase activity associated with IRS-1 and -2. Therefore, insulin signaling in adipose tissue was impaired mainly at the level of IRS-1 and -2 expression. Thus, a high-fat diet apparently causes insulin resistance in the liver by a mechanism different from that causing the insufficient PI 3-kinase activation observed in muscle and adipose tissue.

It is well-known that a diet high in fat tends to cause obesity and leads to both insulin resistance and hyperlipidemia. Our results suggest that the mechanism by which a high-fat diet causes insulin resistance is different from that of abnormality in the leptin system, at least in the liver. Although PI 3-kinase activation is reportedly impaired in the muscle of obese humans, that activation has not been examined in the liver (29). We speculate that alteration of insulin-induced PI 3-kinase activation in the liver depends on whether overeating or a high dietary fat content is primarily responsible for the obesity.

Recently, thiazolidinedione and its derivatives, which enhance insulin action without stimulating β-cell insulin secretion (52–54), have become available for the treatment of NIDDM. These agents bind to peroxisome proliferator-activated receptor-γ and restore the impaired early steps of insulin action preceding PI 3-kinase activation (55–58) and thus have been shown to improve insulin resistance dramatically in several diabetic animal models in which PI 3-kinase activation is impaired—for example, Zucker fatty rats, Zucker diabetic rats, *ob*/*ob* mice, *db*/*db* mice, and KK-Ay mice (59–61). It has also been demonstrated that thiazolidinedione derivatives increase insulin-stimulated PI 3-kinase activity and the amount of p85α associated with IRS-1, without changing the tyrosine phosphorylation of IRS-1 in CHO cells overexpressing insulin receptors and in M6 myotubes (57). In contrast, the insulin-enhancing effects of thiazolidinedione derivatives are rather weak in terms of the insulin resistance induced by a high-fat diet (39). Taking these findings and our liver results into consideration, it is reasonable to speculate that thiazolidinediones cannot improve insulin resistance in the liver of high-fat–fed rats, in which PI 3-kinase activity is already upregulated by some unknown mechanism. As we cannot exclude the possibility that these drugs function not only at the early steps of insulin signaling, but also downstream from the step at which insulin acts, further investigation is needed to resolve the issue.

In summary, we have demonstrated that a high-fat diet affects insulin signaling that induces PI 3-kinase activation differently in liver than in muscle and adipose tissue. In addition, this is the first report showing enhanced PI 3-kinase activa-

tion by insulin in an insulin resistance animal model. These findings may be important for understanding the mechanism of insulin resistance in human NIDDM, since a diet high in fat is recognized as one of the major factors diminishing insulin sensitivity in humans. Our observations may also provide insight into the therapeutic effect of insulin-sensitizing agents on high-fat–induced insulin resistance.

REFERENCES

1. DeFronzo RA, Ferrannini E: Insulin resistance. A multifaceted syndrome responsible for NIDDM, obesity, hypertension, dyslipidemia, and atherosclerotic cardiovascular disease. *Diabetes Care* 14:173–194, 1991
2. Amatruda JM, Livingston JN, Lockwood DH: Cellular mechanisms in selected states of insulin resistance: human obesity, glucocorticoid excess, and chronic renal failure. *Diabetes Metab Rev* 1:293–317, 1985
3. De Pirro R, Green A, Kao MY, Olefsky JM: Effects of prednisolone and dexamethasone in vivo and in vitro: studies of insulin binding, deoxyglucose uptake and glucose oxidation in rat adipocytes. *Diabetologia* 21:149–153, 1981
4. Olefsky JM: Effect of dexamethasone on insulin binding, glucose transport, and glucose oxidation of isolated rat adipocytes. *J Clin Invest* 56:1499–1508, 1975
5. Caro JF, Amatruda JM: Glucocorticoid-induced insulin resistance: the importance of postbinding events in the regulation of insulin binding, action, and degradation in freshly isolated and primary cultures of rat hepatocytes. *J Clin Invest* 69:866–875, 1982
6. Cederholm J, Wibell L: Glucose tolerance and physical activity in a health survey of middle-aged subjects. *Acta Med Scand* 217:373–378, 1985
7. Frisch RE, Wyshak G, Albright TE, Albright NL, Schiff I: Lower prevalence of diabetes in female former college athletes compared with nonathletes. *Diabetes* 35:1101–1105, 1986
8. Seals DR, Hagberg JM, Allen WK, Hurley BF, Dalsky GP, Ehsani AA, Holloszy JO: Glucose tolerance in young and older athletes and sedentary men. *J Appl Physiol* 56:1521–1525, 1984
9. Grundleger ML, Thenen SW: Decreased insulin binding, glucose transport, and glucose metabolism in soleus muscle of rats fed a high fat diet. *Diabetes* 31:232–237, 1982
10. Susini C, Lavau M: In-vitro and in-vivo responsiveness of muscle and adipose tissue to insulin in rats rendered obese by a high-fat diet. *Diabetes* 27:114–120, 1978
11. Storlien LH, James DE, Burleigh KM, Chisholm DJ, Kraegen EW: Fat feeding causes widespread in vivo insulin resistance, decreased energy expenditure, and obesity in rats. *Am J Physiol* 251:E576–E583, 1986
12. Fujimoto WY, Bergstrom RW, Boyko EJ, Kinyoun JL, Leonetti DL, Newell-Morris LL, Robinson LR, Shuman WP, Stolov WC, Tsunehara CH, Wahl PW: Diabetes and diabetes risk factors in second- and third-generation Japanese Americans in Seattle, Washington. *Diabetes Res Clin Pract* 24 (Suppl.):S43–S52, 1994
13. Holbrook TL, Barrett-Connor E, Wingard DL: A prospective population-based study of alcohol use and non-insulin-dependent diabetes mellitus. *Am J Epidemiol* 132:902–909, 1990
14. Thorburn AW, Storlien LH, Jenkins AB, Khouri S, Kraegen EW: Fructose-induced in vivo insulin resistance and elevated plasma triglyceride levels in rats. *Am J Clin Nutr* 49:1155–1163, 1989
15. Cheatham B, Vlahos CJ, Cheatham L, Wang L, Blenis J, Kahn CR: Phosphatidylinositol 3-kinase activation is required for insulin stimulation of pp70 S6 kinase, DNA synthesis, and glucose transporter translocation. *Mol Cell Biol* 14:4902–4911, 1994
16. Kanai F, Ito K, Todaka M, Hayashi H, Kamohara S, Ishii K, Okada T, Hazeki O, Ui M, Ebina Y: Insulin-stimulated GLUT4 translocation is relevant to the phosphorylation of IRS-1 and the activity of PI3-kinase. *Biochem Biophys Res Commun* 195:762–768, 1993
17. Okada T, Kawano Y, Sakakibara T, Hazeki O, Ui M: Essential role of phosphatidylinositol 3-kinase in insulin-induced glucose transport and antilipolysis in rat adipocytes: studies with a selective inhibitor wortmannin. *J Biol Chem* 269:3568–3573, 1994
18. Franke TF, Yang SI, Chan TO, Datta K, Kazlauskas A, Morrison DK, Kaplan DR, Tsichlis PN: The protein kinase encoded by the Akt proto-oncogene is a target of the PDGF-activated phosphatidylinositol 3-kinase. *Cell* 81:727–736, 1995
19. Burgering BM, Coffer PJ: Protein kinase B (c-Akt) in phosphatidylinositol-3-OH kinase signal transduction. *Nature* 376:599–602, 1995
20. Sakaue H, Hara K, Noguchi T, Matozaki T, Kotani K, Ogawa W, Yonezawa K, Waterfield MD, Kasuga M: Ras-independent and wortmannin-sensitive activation of glycogen synthase by insulin in Chinese hamster ovary cells. *J Biol Chem* 270:11304–11309, 1995
21. Shepherd PR, Nave BT, Siddle K: Insulin stimulation of glycogen synthesis and glycogen synthase activity is blocked by wortmannin and rapamycin in 3T3-L1 adipocytes: evidence for the involvement of phosphoinositide 3-kinase and p70 ribosomal protein-S6 kinase. *Biochem J* 305:25–28, 1995
22. Sutherland C, O'Brien RM, Granner DK: Phosphatidylinositol 3-kinase, but not p70/p85 ribosomal S6 protein kinase, is required for the regulation of phosphoenolpyruvate carboxykinase (PEPCK) gene expression by insulin. Dissociation of signaling pathways for insulin and phorbol ester regulation of PEPCK gene expression. *J Biol Chem* 270:15501–15506, 1995
23. Gabbay RA, Sutherland C, Gnudi L, Kahn BB, O'Brien RM, Granner DK, Flier JS: Insulin regulation of phosphoenolpyruvate carboxykinase gene expression does not require activation of the Ras/mitogen-activated protein kinase signaling pathway. *J Biol Chem* 271:1890–1897, 1996
24. Folli F, Saad MJ, Backer JM, Kahn CR: Regulation of phosphatidylinositol 3-kinase activity in liver and muscle of animal models of insulin-resistant and insulin-deficient diabetes mellitus. *J Clin Invest* 92:1787–1794, 1993
25. Saad MJ, Folli F, Kahn CR: Insulin and dexamethasone regulate insulin receptors, insulin receptor substrate-1, and phosphatidylinositol 3-kinase in Fao hepatoma cells. *Endocrinology* 136:1579–1588, 1995
26. Saad MJ, Folli F, Kahn JA, Kahn CR: Modulation of insulin receptor, insulin receptor substrate-1, and phosphatidylinositol 3-kinase in liver and muscle of dexamethasone-treated rats. *J Clin Invest* 92:2065–2072, 1993
27. Carvalho CR, Brenelli SL, Silva AC, Nunes AL, Velloso LA, Saad MJ: Effect of aging on insulin receptor, insulin receptor substrate-1, and phosphatidylinositol 3-kinase in liver and muscle of rats. *Endocrinology* 137:151–159, 1996
28. Saad MJ, Maeda L, Brenelli SL, Carvalho CR, Paiva RS, Velloso LA: Defects in insulin signal transduction in liver and muscle of pregnant rats. *Diabetologia* 40:179–186, 1997
29. Goodyear LJ, Giorgino F, Sherman LA, Carey J, Smith RJ, Dohm GL: Insulin receptor phosphorylation, insulin receptor substrate-1 phosphorylation, and phosphatidylinositol 3-kinase activity are decreased in intact skeletal muscle strips from obese subjects. *J Clin Invest* 95:2195–2204, 1995
30. James DE, Burleigh KM, Kraegen EW: In vivo glucose metabolism in individual tissues of the rat. Interaction between epinephrine and insulin. *J Biol Chem* 261:6366–6374, 1986
31. Ogihara T, Shin BC, Anai M, Katagiri H, Inukai K, Funaki M, Fukushima Y, Ishihara H, Takata K, Kikuchi M, Yazaki Y, Oka Y, Asano T: Insulin receptor substrate (IRS)-2 is dephosphorylated more rapidly than IRS-1 via its association with phosphatidylinositol 3-kinase in skeletal muscle cells. *J Biol Chem* 272:12868–12873, 1997
32. Inukai K, Funaki M, Ogihara T, Katagiri H, Kanda A, Anai M, Fukushima Y, Hosaka T, Suzuki M, Shin BC, Takata K, Yazaki Y, Kikuchi M, Oka Y, Asano T: p85α gene generates three isoforms of regulatory subunit for phosphatidylinositol 3-kinase (PI 3-kinase), p50α, p55α and p85α, with different PI 3-kinase activity elevating responses to insulin. *J Biol Chem* 272:7873–7882, 1997
33. Anai M, Funaki M, Ogihara T, Terasaki J, Inukai K, Katagiri H, Fukushima Y, Yazaki Y, Kikuchi M, Oka Y, Asano T: Altered expression levels and impaired steps in the pathway to phosphatidylinositol 3-kinase activation via IRS-1 and IRS-2 in Zucker fatty rats. *Diabetes* 47:13–23, 1998
34. Caro JF, Dohm LG, Pories WJ, Sinha MK: Cellular alterations in liver, skeletal muscle, and adipose tissue responsible for insulin resistance in obesity and type II diabetes. *Diabetes Metab Rev* 5:665–689, 1989
35. White MF, Kahn CR: The insulin signaling system. *J Biol Chem* 269:1–4, 1994
36. Kahn CR, Folli F: Molecular determinants of insulin action. *Horm Res* 39 (Suppl. 3):93–101, 1993
37. Clarke JF, Young PW, Yonezawa K, Kasuga M, Holman GD: Inhibition of the translocation of GLUT1 and GLUT4 in 3T3-L1 cells by the phosphatidylinositol 3-kinase inhibitor, wortmannin. *Biochem J* 300:631–635, 1994
38. Kraegen EW, Clark PW, Jenkins AB, Daley EA, Chisholm DJ, Storlien LH: Development of muscle insulin resistance after liver insulin resistance in high-fat-fed rats. *Diabetes* 40:1397–1403, 1991
39. Khoursheed M, Miles PD, Gao KM, Lee MK, Moossa AR, Olefsky JM: Metabolic effects of troglitazone on fat-induced insulin resistance in the rat. *Metab Clin Exper* 44:1489–1494, 1995
40. Kraegen EW, James DE, Storlien LH, Burleigh KM, Chisholm DJ: In vivo insulin resistance in individual peripheral tissues of the high fat fed rat: assessment by euglycaemic clamp plus deoxyglucose administration. *Diabetologia* 29:192–198, 1986
41. Maegawa H, Kobayashi M, Ishibashi O, Takata Y, Shigeta Y: Effect of diet change on insulin action: difference between muscles and adipocytes. *Am J Physiol* 251:E616–E623, 1986
42. Traianedes K, Proietto J, O'Dea K: A high-fat diet worsens metabolic control in streptozotocin-treated rats by increasing hepatic glucose production. *Metabolism* 41:846–850, 1992

43. Zaragoza-Hermans N, Felber JP: Studies on the metabolic effects induced in the rat by a high-fat diet: (U-^{14}C) glucose metabolism in epididymal adipose tissue. *Eur J Biochem* 25:89–95, 1972
44. Zierath JR, Houseknecht KL, Gnudi L, Kahn BB: High-fat feeding impairs insulin-stimulated GLUT4 recruitment via an early insulin-signaling defect. *Diabetes* 46:215–223, 1997
45. Ozanne SE, Nave BT, Wang CL, Shepherd PR, Prins J, Smith GD: Poor fetal nutrition causes long-term changes in expression of insulin signaling components in adipocytes. *Am J Physiol* 273:E46–E51, 1997
46. Shepherd PR, Nave BT, Rincon J, Nolte LA, Bevan AP, Siddle K, Zierath JR, Wallberg-Henriksson H: Differential regulation of phosphoinositide 3-kinase adapter subunit variants by insulin in human skeletal muscle. *J Biol Chem* 272:19000–19007, 1997
47. Sun XJ, Crimmins DL, Myers MG Jr, Miralpeix M, White MF: Pleiotropic insulin signals are engaged by multisite phosphorylation of IRS-1. *Mol Cell Biol* 13:7418–7428, 1993
48. Sun XJ, Wang LM, Zhang Y, Yenush L, Myers MG Jr, Glasheen E, Lane WS, Pierce JH, White MF: Role of IRS-2 in insulin and cytokine signalling. *Nature* 377:173–177, 1995
49. Myers MG Jr, White MF: The new elements of insulin signaling: insulin receptor substrate-1 and proteins with SH2 domains. *Diabetes* 42:643–650, 1993
50. Carpenter CL, Auger KR, Duckworth BC, Hou WM, Schaffhausen B, Cantley LC: A tightly associated serine/threonine protein kinase regulates phosphoinositide 3-kinase activity. *Mol Cell Biol* 13:1657–1665, 1993
51. Dhand R, Hiles I, Panayotou G, Roche S, Fry MJ, Gout I, Totty NF, Truong O, Vicendo P, Yonezawa K, Kasuga M, Courtneidge SA, Waterfield MD: PI 3-kinase is a dual specificity enzyme: autoregulation by an intrinsic protein-serine kinase activity. *EMBO J* 13:522–533, 1994
52. Antonucci T, Whitcomb R, McLain R, Lockwood D: Impaired glucose tolerance is normalized by treatment with the thiazolidinedione troglitazone. *Diabetes Care* 20:188–193, 1997
53. Kumar S, Boulton AJ, Beck-Nielsen H, Berthezene F, Muggeo M, Persson B, Spinas GA, Donoghue S, Lettis S, Stewart-Long P: Troglitazone, an insulin action enhancer, improves metabolic control in NIDDM patients: Troglitazone Study Group. *Diabetologia* 39:701–709, 1996 (Erratum published in *Diabetologia* 39:1245, 1996)
54. Chaiken RL, Eckert-Norton M, Pasmantier R, Boden G, Ryan I, Gelfand RA, Lebovitz HE: Metabolic effects of darglitazone, an insulin sensitizer, in NIDDM subjects. *Diabetologia* 38:1307–1312, 1995
55. Terasaki J, Anai M, Funaki M, Shibata T, Inukai K, Ogihara T, Ishihara H, Katagiri H, Onishi Y, Sakoda H, Fukushima Y, Yazaki Y, Kikuchi M, Oka Y, Asano T: Role of JTT-501, a new insulin sensitiser, in restoring impaired GLUT4 translocation in adipocytes of rats fed a high fat diet. *Diabetologia* 41:400–409, 1998
56. Lehmann JM, Moore LB, Smith-Oliver TA, Wilkison WO, Willson TM, Kliewer SA: An antidiabetic thiazolidinedione is a high affinity ligand for peroxisome proliferator-activated receptor gamma (PPAR gamma). *J Biol Chem* 270:12953–12956, 1995
57. Zhang B, Szalkowski D, Diaz E, Hayes N, Smith R, Berger J: Potentiation of insulin stimulation of phosphatidylinositol 3-kinase by thiazolidinedione-derived antidiabetic agents in Chinese hamster ovary cells expressing human insulin receptors and L6 myotubes. *J Biol Chem* 269:25735–25741, 1994
58. Kobayashi M, Iwanishi M, Egawa K, Shigeta Y: Pioglitazone increases insulin sensitivity by activating insulin receptor kinase. *Diabetes* 41:476–483, 1992
59. Young PW, Cawthorne MA, Coyle PJ, Holder JC, Holman GD, Kozka IJ, Kirkham DM, Lister CA, Smith SA: Repeat treatment of obese mice with BRL 49653, a new potent insulin sensitizer, enhances insulin action in white adipocytes: association with increased insulin binding and cell-surface GLUT4 as measured by photoaffinity labeling. *Diabetes* 44:1087–1092, 1995
60. Zhang B, Graziano MP, Doebber TW, Leibowitz MD, White-Carrington S, Szalkowski DM, Hey PJ, Wu M, Cullinan CA, Bailey P, Lollmann B, Frederich R, Flier JS, Strader CD, Smith RG: Down-regulation of the expression of the obese gene by an antidiabetic thiazolidinedione in Zucker diabetic fatty rats and db/db mice. *J Biol Chem* 271:9455–9459, 1996
61. Sizer KM, Smith CL, Jacob CS, Swanson ML, Bleasdale JE: Pioglitazone promotes insulin-induced activation of phosphoinositide 3-kinase in 3T3-L1 adipocytes by inhibiting a negative control mechanism. *Mol Cell Endocrinol* 103:1–12, 1994

Author Queries (please see Q in margin and underlined text)

Q1: Please supply a mailing address for correspondence.
Q2: Please supply city in Japan for Nippon Gene.
Q3: Correct that you meant approximately (~) 800 Ci, as opposed to negative (–) 800 Ci?
Q4: Please clarify—there are no * (asterisks) or ** (double asterisks) in figure 2.
Q5: Please clarify—there are no single asterisks (*) in figure 5.
Q6: Please cite figure 8 in the text.
Q7: Please define/spell out MBL.
Q8: Please define/spell out NEN. If it represents a manufacturer, also provide the address of the manufacturer, including the city and state or country.
Q9: Please define/spell out HGP. (CJP: Add to abbreviations.)

Please supply all authors' names for Ref. 12.